

Aminochrome Induces Disruption of Actin, Alpha-, and Beta-Tubulin Cytoskeleton Networks in Substantia-Nigra-Derived Cell Line

Irmgard Paris · Carolina Perez-Pastene · Sergio Cardenas · Patricio Iturra · Patricia Muñoz · Eduardo Couve · Pablo Caviedes · Juan Segura-Aguilar

Received: 15 September 2009 / Revised: 19 November 2009 / Accepted: 23 December 2009 / Published online: 20 January 2010
© Springer Science+Business Media, LLC 2010

Abstract In previous studies, we observed that cells treated with aminochrome obtained by oxidizing dopamine with oxidizing agents dramatically changed cell morphology, thus posing the question if such morphological changes were dependent on aminochrome or the oxidizing agents used to produce aminochrome. Therefore, to answer this question, we have now purified aminochrome on a CM-Sepharose 50–100 column and, using NMR studies, we have confirmed that the resulting aminochrome was pure and that it retained its structure. Fluorescence microscopy with calcein-AM and transmission electron microscopy showed that RCSN-3 cells presented an elongated shape that did not change when the cells were

incubated with 50 µM aminochrome or 100 µM dicoumarol, an inhibitor of DT-diaphorase. However, the cell were reduced in size and the elongated shape become spherical when the cells where incubated with 50 µM aminochrome in the presence of 100 µM dicoumarol. Under these conditions, actin, alpha-, and beta-tubulin cytoskeleton filament networks became condensed around the cell membrane. Actin aggregates were also observed in cells processes that connected the cells in culture. These results suggest that aminochrome one-electron metabolism induces the disruption of the normal morphology of actin, alpha-, and beta-tubulin in the cytoskeleton, and that DT-diaphorase prevents these effects.

Keywords Actin · Tubulin · Aminochrome · Dopamine · Cytoskeleton · Cell shrinkage · DT-diaphorase

Irmgard Paris and Carolina Perez-Pastene should be considered as primer author of this work.

Please address all correspondence regarding the use of the RCSN3 cell line to Pablo Caviedes. e-mail: pcaviede@med.uchile.cl

I. Paris · C. Perez-Pastene · S. Cardenas · P. Muñoz ·
P. Caviedes · J. Segura-Aguilar (✉)
Program of Molecular and Clinical Pharmacology, Faculty
of Medicine, ICBM, Independencia 1027, Casilla,
Santiago 70000, Chile
e-mail: jsegura@med.uchile.cl

P. Iturra
Department of Chemistry, Faculty of Sciences,
University of Chile, Santiago, Chile

I. Paris
Universidad Santo Tomás, Vina del Mar, Chile

E. Couve
University of Valparaíso, Valparaíso, Chile

Introduction

The discovery that mutated alpha-synuclein was associated with a familiar form of Parkinson's disease (Polymeropoulos et al. 1997) opened a new field of research focused in understanding the role of alpha-synuclein in sporadic Parkinson's disease (Buchman and Ninkina 2008a, b; Sulzer et al. 2008; Fernández 2008; Duka and Sidhu 2006). Mutated alpha-synuclein induces the formation of non-fibrillar alpha-synuclein oligomers, characterized as spheres, chains of spheres (protofibrils), and rings resembling circularized protofibrils (Conway et al. 2000). Formation of neurotoxic protofibrils is enhanced and stabilized by dopamine quinones derived from the oxidation of dopamine, thus accounting for the selective toxicity of alpha-synuclein protofibrils in the substantia nigra (Conway et al. 2001). However, aminochrome was

found to be the dopamine quinone species responsible for the induction and stabilization of neurotoxic profibrils (Norris et al. 2005). Further, aminochrome was found to affect the axonal transport of alpha-synuclein (Riveros et al. 2008).

The degeneration and loss of neuromelanin-containing dopaminergic neurons in Parkinson's disease suggests that dopamine oxidation to aminochrome is an intracellular event which probably plays a role in the degenerative process in this disease. The oxidation of dopamine to dopamine *o*-quinone at physiological pH levels is followed by the spontaneous amino chain cyclization in several steps to form aminochrome, a precursor of neuromelanin (Segura-Aguilar and Lind 1989). It has been proposed that aminochrome could be the neurotoxin involved in the neurodegeneration of dopaminergic neurons containing neuromelanin in Parkinson's disease, and therefore, aminochrome has been proposed as a more physiological preclinical model than 6-hydroxydopamine or MPTP in the study of the neurodegenerative mechanism of dopaminergic neurons in PD (Paris et al. 2007).

In previous studies, we demonstrated the effect of aminochrome in RCSN-3 cells using different oxidizing agents such as manganese(III), copper(II), iron(III) or in the presence of the VMAT-2 inhibitor reserpine (Paris et al. 2001, 2005a, b, 2009a; Arriagada et al. 2004; Fuentes et al. 2007). Interestingly, in these experiments, we observed that the cells undergo a dramatic morphological change. Therefore, the aim of this study is to study aminochrome-induced morphological changes, this time using a purified aminochrome, in order to clearly assess the effect of this compound in this *in vitro* dopaminergic cellular model.

Materials and Methods

Chemicals

Dopamine, dicoumarol, menadione, DME/HAM-F12 nutrient mixture (1:1), Hank's solution, were purchased from Sigma Chemical Co. (St Louis, MO, USA). Vector GFP-LC3 was a kind gift from Zsolt Talloky Ph.D., Columbia University Medical Center. LIVE/DEAD Viability/Cytotoxicity Kit, Molecular Probes (Eugene, OR, USA). Antibody mouse monoclonal anti- α -Tubulin and goat polyclonal anti- α actin were purchased from Santa Cruz Biotechnology, CA, USA. Biotinylated anti-mouse and Biotinylated anti-goat were purchased from Vector Laboratories, Burlingame, CA, USA. CyTM-3-conjugated streptavidin were purchased from Jackson ImmunoResearch Laboratories, West Grove, PA, USA.

Aminochrome Synthesis and Purification

Aminochrome synthesis was performed by oxidizing 5 mM dopamine with 10 ng tyrosinase in buffer 20 mM MES at pH 6.0 for 15 min at room temperature. Aminochrome was separated from unreacted dopamine and tyrosinase with a CM-Sephadex C50-100 column (18 × 0.7 cm) equilibrated with 20 mM MES at pH 6.0. The elution of the column was monitored by recording the absorbance at 280 nm, as tyrosinase, unreacted dopamine, and aminochrome have a maximal absorption at this wavelength, and at 475 nm, where aminochrome alone has a maximal absorption maximum at this wavelength. Aminochrome was eluted by adding 7 ml 20 mM MES at pH 6.0, with a yield of approximately 220 μ M pure aminochrome in 1.5 ml buffer. Aminochrome was then analyzed using NMR and absorption spectra between 200 and 800 nm. Not reacted dopamine was eluted with a pulse of 300 mM NaCl in 20 mM MES at pH 6.0. The concentration of aminochrome was determined using the molar extinction coefficient 3058 $M^{-1} \text{cm}^{-1}$ (Segura-Aguilar and Lind 1989).

NMR Spectroscopy

For the structural analysis of aminochrome in deuterium oxide, the $^1\text{H-NMR}$ spectrum was recorded using a π -gradient Bruker Avance 400 instrument, operating at 400 MHz with suppression of the water signal. The pulse program was zg-30 and the duration of the experiment was 300 min.

Cell Culture

The RCSN-3 cell line grows in monolayers, with a doubling time of 52 h, a plating efficiency of 21% and a saturation density of 56,000 cells/cm² in normal growth media composed of DME/HAM-F12 (1:1), 10% bovine serum, 2.5% fetal bovine serum, 40 mg/l gentamicin sulfate (Paris et al. 2008a). The cultures were kept in an incubator at 37°C with 100% humidity, and the cells were grown in atmospheres of both 5 or 10% CO₂ (Paris et al. 2008a, b, 2009a, b). The cell morphology was determined by staining the cells with 0.5 μ M Calcein AM for 45 min at room temperature in the dark (Molecular Probes). The cell morphology was determined by using a phase contrast microscope equipped with fluorescence using the following filters: 450–490 nm (excitation) and 515–565 nm (emission).

Incubations

In all experiments performed in this study, we incubated RCSN-3 cells with 50 μ M aminochrome in the absence or

presence of 100 μM dicoumarol. For control conditions, the cells were incubated with 100 μM dicoumarol or the solely with culture medium.

Transmission Electron Microscopy

Cells incubated as described above were pelleted and fixed with 3% glutaraldehyde in 0.1-M cacodylate buffer pH 7.4 for 120 min, washed three times, and post-fixed in osmium tetroxide 1% for 60 min. The cells were dehydrated in an ascending ethanol battery ranging from 20 to 100%, and were later placed in 3:1, 2:1, 1:1, 1:2, 1:3 ratios of propylene oxide or epom-812 resin for 1 h at room temperature, respectively. Ultrathin sections of 70 nm were made and impregnated with 2% uranyl acetate and Reynold's lead citrate. The sections were visualized in a Zeiss EM-900 transmission electron microscope at 50 kV and photographed. The negatives were scanned at 600 \times 600 dpi resolution, and the images obtained were later analyzed with a PC-compatible computer using customized software.

Immunofluorescence Analysis with Confocal Microscopy

Coverslips containing control RCSN-3 cells grown to 50% confluence were washed twice with Dulbecco's PBS, pH 7.4. They were then fixed for 30 min with methanol at -20°C . The cells were rinsed twice with TBS and blocked with 1% bovine serum albumin diluted (BSA) in TBS for 60 min. The blocking solution was then aspirated and the cells were rinsed with TBS. The coverslips were incubated with the primary antibody (mousse monoclonal anti- α -Tubulin, 1:250; goat polyclonal anti- α actin, 1:100) in 1% BSA during overnight. The primary antibody was aspirated, and the cells were washed 10 times with TBS. After washing, the cells were incubated for 2 h with secondary antibody (Biotinylated anti-mouse; Biotinylated anti-goat; Vector Laboratories, Burlingame, CA, USA) diluted 1:250 in TBS. The secondary antibody was removed and the cells were washed 10 times with TBS. The cells were incubated with CyTM-3-conjugated streptavidin 1.5 $\mu\text{g}/\text{ml}$ (Jackson ImmunoResearch Laboratories, West Grove, PA, USA) for 1 h to room temperature. The streptavidin solution was removed and cells were washed 10 times with TBS. Coverslips were mounted onto slides with fluorescent mounting medium (Dako, Carpinteria, CA, USA) and kept in the dark at 4°C . Confocal microscopy (Zeiss, Göttingen, Germany; model LSM-410 Axiovert-100) was used to study the cells. Sample illumination was carried out via a He-Ne laser with 543 nm excitation filter and emission filter over 560 nm.

Determination of Aminochrome K_M

The Michaelis constant (K_M) was determined in Tris/HCl buffer at pH 7.5 containing 0.08% Triton X-100, 500 μM NADH, 38-nM DT-diaphorase and 0–100 μM aminochrome at 37°C . The aminochrome K_M was calculated by a Lineweaver–Burk plot.

Determination of Quinone Reductase Activity

The quinone reductase activity in RCSN-3 cells was determined in Tris/HCl buffer at pH 7.5 containing 0.08% Triton X-100 by using 500 μM NADH or 500 μM NADPH as electron donor, 77 μM cytochrome c and 10 μM menadione as electron acceptor. The reaction was measured spectrophotometrically by following the reduction of cytochrome c, which continuously reoxidize the reduced menadione, at 550 nm and employing an extinction coefficient of $18.5 \text{ mM}^{-1} \text{ cm}^{-1}$. DT-diaphorase activity was calculated by inhibiting the quinone reductase activity with dicoumarol.

Results

We purified aminochrome to avoid the possible interference of oxidizing agents present during aminochrome synthesis, in the present studies on aminochrome effects on cell morphology. Aminochrome was generated by oxidizing 5 mM dopamine with 10 ng tyrosinase in buffer 20 mM MES at pH 6.0 during 15 min. This solution was loaded on a CM-Sephadex C50-100 column and the elution was initiated with 20 mM MES at pH 6.0, whereas the absorbance was monitored at 280 and 475 nm. Tyrosinase passed through the column without any interaction with the column, but aminochrome was delayed and eluted at 7 ml with the same buffer. This peak (I) was completely separated from tyrosinase, exhibiting absorbance both at 280 and at 475 nm and the yield of aminochrome was 500 μM . Not reacted dopamine was bound to the column and it was not eluted until we applied 300 mM NaCl in 20 mM MES at pH 6.0. This peak (II), which eluted at 15 ml, exhibited absorbance at 280 nm (Fig. 1a). The peak II was identified as dopamine by comparing its absorption spectrum with the spectrum of pure dopamine and in addition, this pool could be oxidized to aminochrome by tyrosinase, as determined by spectrophotometry. The absorption spectrum of pure aminochrome exhibited three peaks at 220, 287, and 477 nm (Fig. 1b). Aminochrome stability was pH-dependent since at pH 6.0 and 7.4 the 50% decay was at 112 and 183 min, respectively. The ¹H-NMR spectrum of the aminochrome showed clear differences between the aromatic proton resonance pattern of dopamine and that of its

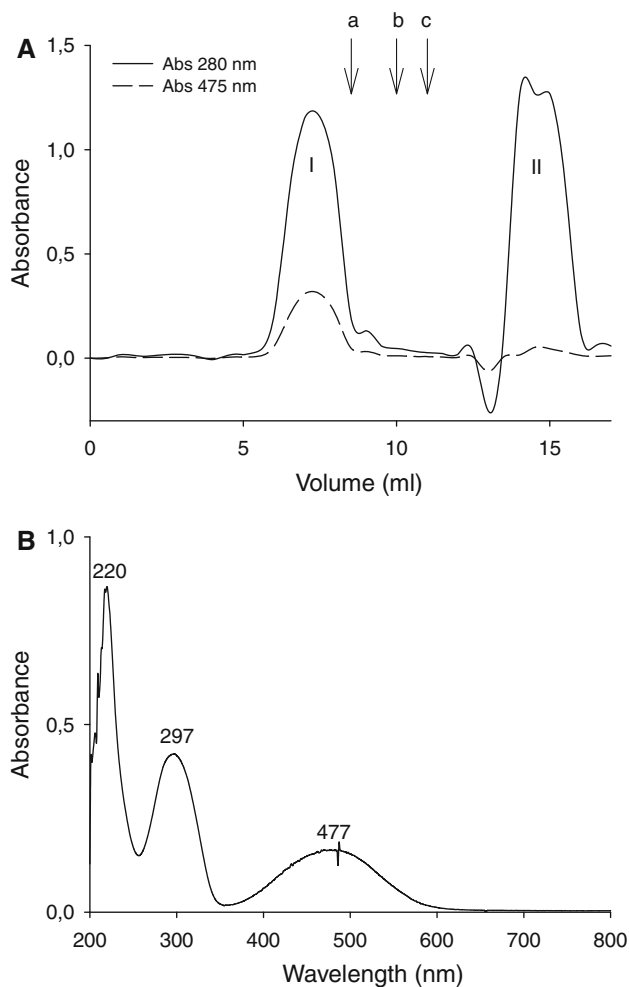


Fig. 1 Aminochrome purification. **a** A solution of 500 μ l containing aminochrome, tyrosinase, and unreacted dopamine was applied to CM-Sepharose C50-100 column equilibrated with 20 mM MES at pH 6.0. The elution of the column was monitored at 280 and 475 nm, as described under Experimental Procedures. The elution of dopamine was performed by adding 20 mM MES at pH 6.0 containing 100 μ M (arrow *a*), 200 μ M (arrow *b*), and 300 mM NaCl (arrow *c*). **b** The spectrum of pure aminochrome was done with 20 mM MES at pH 6.0

oxidative metabolite aminochrome. Dopamine showed three aromatic protons with a characteristic ABM coupling pattern, while aminochrome showed only two protons in the aromatic proton resonance range. Both signals in the aminochrome spectrum and the lack of one aromatic proton signal are in agreement with the structure proposed for the cyclic aminochrome metabolite. Two protons resonating at 6.41 (H-4) and 5.57 (H-7) ppm could be observed for the *o*-quinone moiety and, if we compare the aromatic protons in the dopamine spectrum, those are evident at 6.41 (1H) and 6.51 (2H) ppm. The upfield for H-7 (5.57 ppm) in the aminochrome could be correlated with the cyclic dopamine *o*-quinone. The H-4 proton has an unusual long-range coupling ($J_4 = 2.57$ Hz) with the H-3 methylene protons of the pyrrolidine ring, which could be explained by the

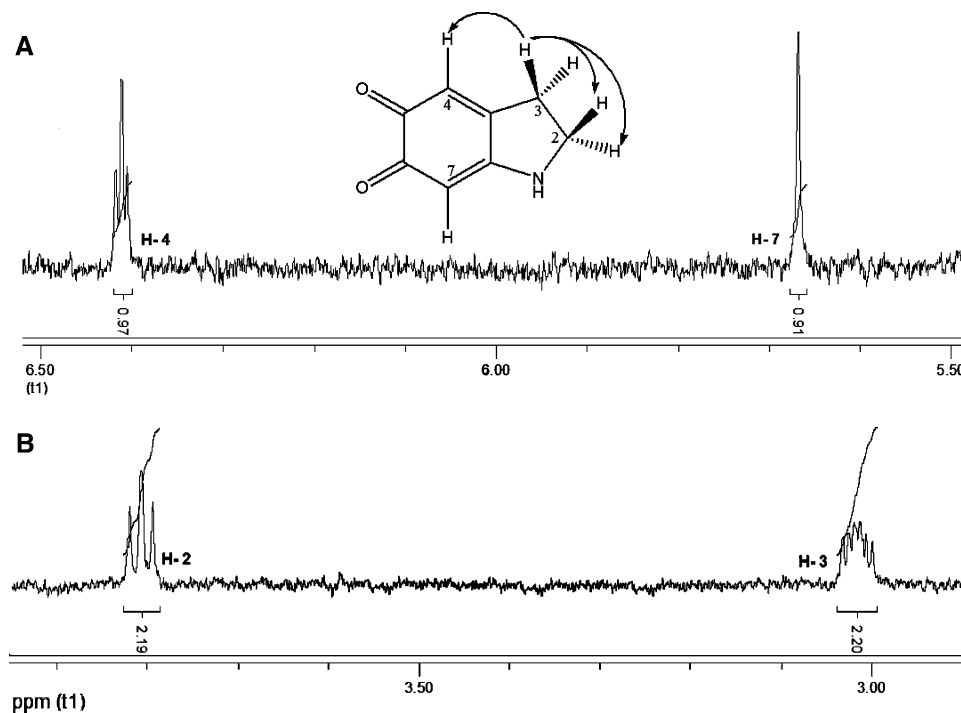
loss of flexibility on dopamine ethylene amino moiety. The pyrrolidine ring gave two different methylene group resonances: H-2 (3.81 ppm; $J_3 = 5.18$ Hz), which exhibited a typical vicinal triplet coupling pattern with the H-3 methylene. However, the H-3 (3.02 ppm) methylene protons gave rise to a multiplet with two different coupling systems with $J_3 = 5.19$ Hz and $J_4 = 2.55$ Hz, where one corresponds to the long-range couplings with H-4 in the *o*-quinone ring (Fig. 2). 2,3-dihydro-1H-indole-5,6-dione (aminochrome) 1H-NMR (D_2O) δ 3.02 (dd, 2H, $J_3 = 5.19$, $J_4 = 2.55$ Hz), 3.81 (t, 2H, $J_3 = 5.18$ Hz), 5.57 (s, 1H), 6.41 (t, 1H, $J_4 = 2.57$ Hz). 2-(3,4-dihydroxyphenyl)ethylamine (dopamine) 1H-NMR (D_2O) δ 2.81 (t, 2H, $J_3 = 4.78$ Hz), 2.98 (t, 2H, $J_3 = 4.67$ Hz), 6.42 (s, 1H), 6.51 (s, 2H). The K_M of pure aminochrome for DT-diaphorase calculated by a Lineweaver-Burk plot was 170 nM.

We determined the quinone reductase activity in RCSN-3 cells to study aminochrome effect on RCSN-3 cells. DT-diaphorase activity in RCSN-3 cells was 1.42 and 1.18 μ mol/min/mg protein using NADPH and NADH as electron donors, while the quinone reductase activity catalyzed by flavoenzymes that use NADPH or NADH as electron donors was 10 and 14 nmol/min/mg protein total quinone reductase, respectively. The incubation of RCSN-3 cells with 50 μ M aminochrome and 100 μ M dicoumarol for 24 h induced a dramatic change in cell morphology. The elongated cell shape observed in control cells incubated with cell culture medium alone (Fig. 3-I a) did not change when the cells were treated with 100 μ M dicoumarol (Fig. 3b) or 50 μ M aminochrome alone (Fig. 3-I c). However, in the presence of 50 μ M aminochrome and 100 μ M dicoumarol, the elongated cell shape underwent a dramatic change, expressed in the reduction of cell size, and the onset of a spherical shape (Fig. 3-I d).

Transmission electron microscopy confirmed that RCSN-3 cells incubated with 50 μ M aminochrome and 100 μ M dicoumarol were reduced in size, lose their elongated shape to become spherical (Fig. 3-I d), contrasting with the elongated shape of control cells incubated with cell culture medium or cells incubated with 50 μ M aminochrome or 100 μ M dicoumarol during 24 h (Fig. 3-II a-c).

The dramatic change in cell morphology induced by aminochrome in the presence of dicoumarol opened the question about the possibility that aminochrome could be affecting the cytoskeleton. Therefore, we decided to study the possible effect of aminochrome on actin, alpha-, and beta-tubulin filaments using immunostaining techniques in cells incubated with the treatment detailed above for 24 h. No changes in actin filaments was observed in cells treated with 50 μ M aminochrome or 100 μ M dicoumarol when compared to control cells incubated solely with cell culture medium. However, the change in cell shape was accompanied by a disruption of the actin filament network when

Fig. 2 Aminochrome ^1H -NMR spectrum (400 MHz) in D_2O . **a** Aromatic proton region showing H-4 and H-7 protons and **b** methylene proton region showing H-2 and H-3 protons. The conditions are described under Experimental Procedures



the cells were incubated with 50 μM aminochrome and 100 μM dicoumarol. The actin filaments seemed to form aggregates that surrounded the cell membrane (Fig. 4d, f). Interestingly, RCSN-3 cell processes that connect the cells in the cell culture medium, presented actin aggregates when the cells were incubated with 50 μM aminochrome and 100 μM dicoumarol (Fig. 4e). Immunostaining using specific antibodies against alpha-tubulin confirmed the disruption of the alpha-tubulin filament network and the formation of aggregates around the cell membrane when the cells were incubated with 50 μM aminochrome and 100 μM dicoumarol (Fig. 5d).

Finally, beta-tubulin also aggregated around the cell membrane in cells incubated with 50 μM aminochrome and 100 μM dicoumarol. However, no changes were observed when the cells were incubated with cell culture medium, 50 μM aminochrome or 100 μM dicoumarol (not shown).

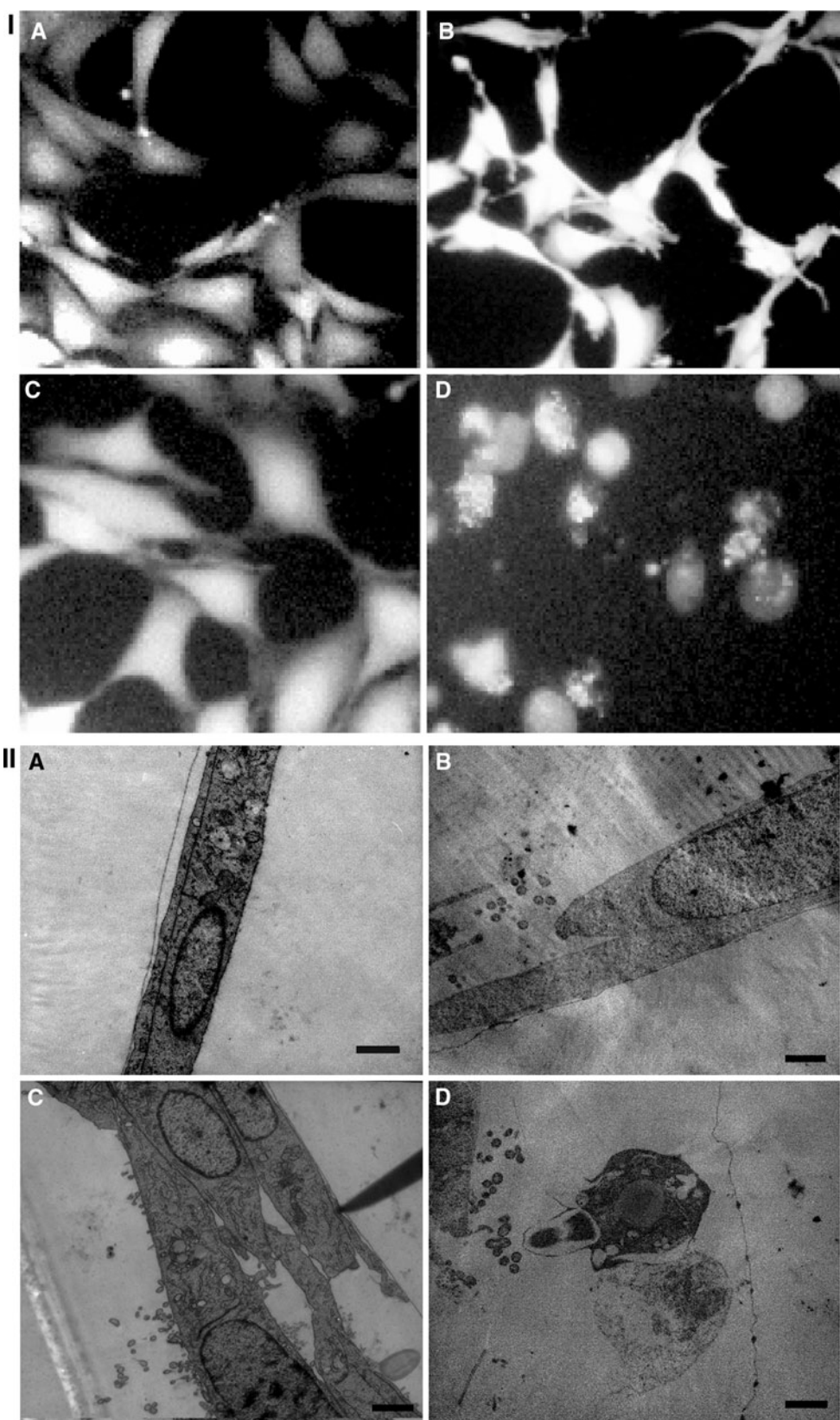
Discussion

Neuromelanin-containing neurons are lost during the neurodegenerative process underlying Parkinson's disease. Aminochrome is the precursor of neuromelanin, and it is formed during dopamine oxidation. Oxygen catalyzes dopamine oxidation to dopamine *o*-quinone, which automatically cyclizes in several steps to form aminochrome at physiological pH level. Oxidation of dopamine to aminochrome is also catalyzed by enzymes (prostaglandin H

synthase, cytochrome P450 forms, xanthine oxidase, tyrosinase, and dopamine *b*-monooxygenase or transition metals; Paris et al. 2001, 2005a; Hastings 1995; Segura-Aguilar and Lind 1989; Gauthier et al. 2008). Further, aminochrome can participate in several reactions. (i) The first reaction is the polymerization to form neuromelanin that accumulates with age in the human substantia nigra (Zecca et al. 2002, 2008). (ii) The second reaction undergone by aminochrome is the formation of protein adducts such as alpha-synuclein. Aminochrome inhibits alpha-synuclein fibrillization and enhances and stabilizes the formation of neurotoxic protofibrils (Norris et al. 2005; Conway et al. 2001). (iii) Aminochrome can also be reduced by one electron to form the neurotoxic leukoaminochrome-*o*-semiquinone radical, which is extremely reactive with oxygen. This reaction can be catalyzed by flavoenzymes that reduce quinones with one-electron (Baez et al. 1995; Segura-Aguilar et al. 1998). (iv) Aminochrome can be reduced by two electrons to form leukoaminochrome, a process which is catalyzed by DT-diaphorase. This process prevents aminochrome from participating in two neurotoxic reactions to form leukoaminochrome *o*-semiquinone radicals through the one-electron reduction of aminochrome and prevents the formation of neurotoxic protofibrils during the formation of aminochrome adducts with alpha-synuclein (Paris et al. 2001, 2005a, b, 2008b, 2009a; Arriagada et al. 2004; Segura-Aguilar et al. 2006; Cardenas et al. 2008a, b).

Aminochrome is able to tautomerize to indole-5,6-quinone and therefore, the question is whether indole-5,6-quinone or aminochrome is the species relevant during

Fig. 3 RCSN-3 cells morphology in the presence of aminochrome. The cells were treated with cell culture medium (**a**); 100 μ M dicoumarol (**b**); 50 μ M aminochrome (**c**); and 50 μ M aminochrome and 100 μ M dicoumarol (**d**) during 48 h and the morphology was determined by using a phase contrast microscope equipped with fluorescence (I) and transmission electron microscopy (II)



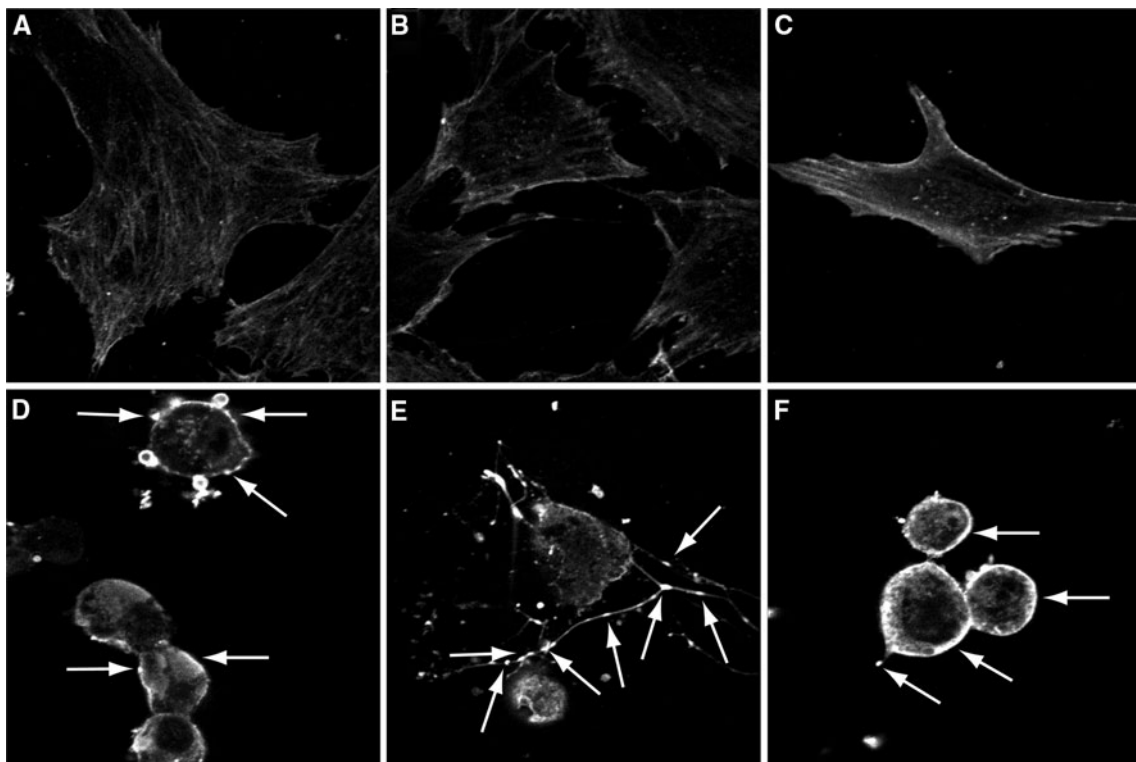


Fig. 4 The effect of aminochrome on actin in RCSN-3 cells. The effect of aminochrome on actin in RCSN-3 cells were determined by using confocal microscopy. The cells were treated with cell culture

medium (**a**); 100 μ M dicoumarol (**b**); 50 μ M aminochrome (**c**) and 50 μ M aminochrome and 100 μ M dicoumarol (**d–f**) during 48 h. The arrows show actin aggregation

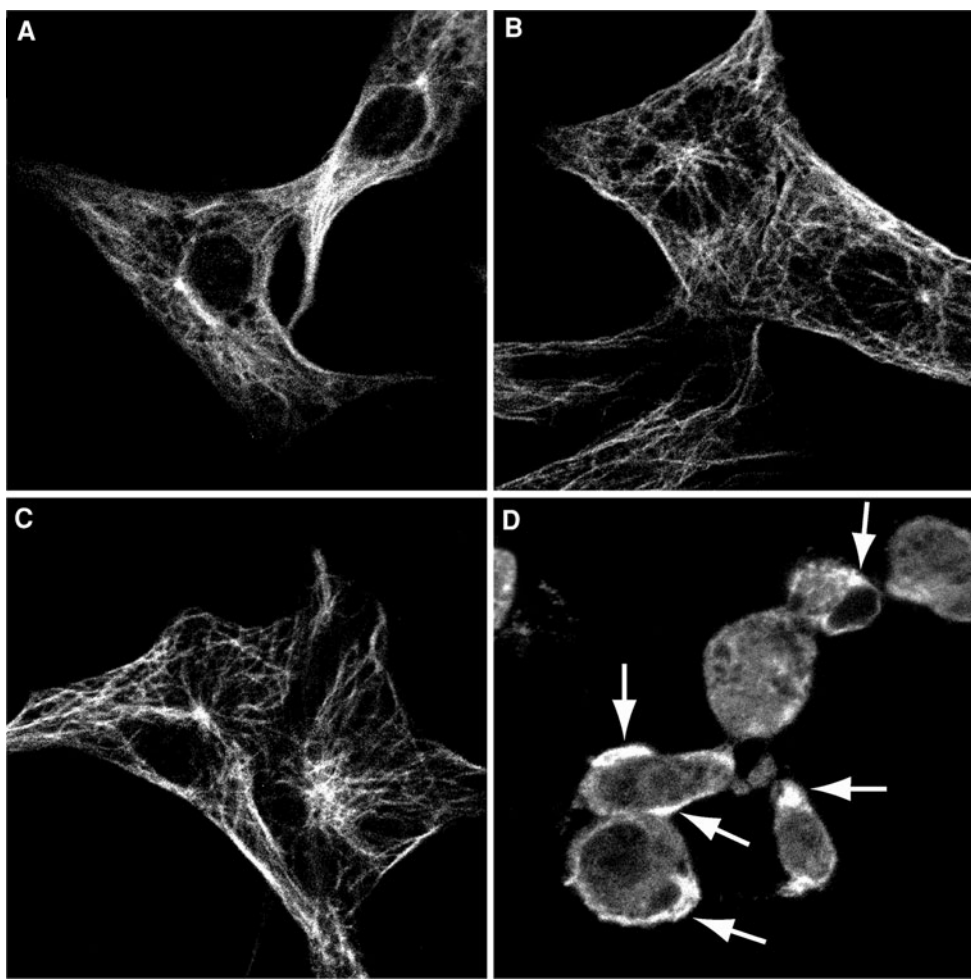
dopamine oxidation at physiological conditions in dopaminergic neurons. According to other studies, aminochrome was 100% converted to 5,6-dihydroxyindole (precursor of indole-5,6-quinone) after 20 min incubation when aminochrome was formed by oxidizing dopamine with NaIO₄ (1–4 mM), (Bisaglia et al. 2007). However, purified aminochrome is more stable at physiological pH 7.4 since the 50% decay was observed at 112 min. Therefore, purified aminochrome under intracellular conditions is more than enough stable to be metabolized by flavoenzymes where the transfer of electrons are extremely rapid supporting the idea that aminochrome is the species relevant at physiological pH. Another result supporting this idea was that aminochrome conjugation with GSH catalyzed by glutathione transferase M2-2 resulted in the formation of 4-S-glutathionyl-5,6-dihydroxyindoline and not the conjugated form of indole-5,6-quinone (4-S-glutathionyl-5,6-dihydroxyindole) (Segura-Aguilar et al. 1997).

In the present study, we present a methodology to produce pure aminochrome from dopamine and the oxidizing agents used to oxidize dopamine. The comparison of aminochrome with the corresponding *O,O*-diacetylcyclodopa spectrum (Büchi and Kamikawa 1977) showed that the H-7 proton (6.55 ppm) in the cyclodopa appears downfield to the corresponding proton in aminochrome. In the *O,O*-diacetylcyclodopa, the H-7 proton is closer to the

dopamine aromatic proton than that of H-7 in aminochrome. The upfield exhibited by H-7 could be associated with an aminochrome *o*-quinone moiety, which is characteristic for non-aromatic protons in *o*-quinones. Similar comparisons have been made for urushiol (a catecholic compound) and its *o*-quinone tautomer, where the hydrogen resonance for the carbonyl neighboring proton suffers an upfield displacement (6.3 ppm) in contrast with the hydrogen in the catecholic tautomers (6.7 ppm) (Liberato et al. 1981) Indeed, analysis of the urushiols suggests that our aminochrome metabolite corresponds with the *o*-quinone structure. In light of these results, we can state that the aminochrome structure was confirmed by the ¹H-NMR spectrum (Fig. 2). In addition, our NMR results with purified aminochrome are in agreement with studies with aminochrome formed by oxidizing dopamine with NaIO₄ (Bisaglia et al. 2007).

Eukaryotic cells contain a 3-dimensional cytoskeleton network formed by microfilaments, microtubules, and intermediate filaments. Microfilaments are composed of actin polymers which are in dynamic equilibrium with globular actin monomers. Actin is an important component of the cellular cytoskeleton, which is essential for sculpting and maintaining cell shape (Cingolani and Goda 2008). Actin is present at the synaptic terminals and therefore, it has been proposed that actin is involved in maintaining and

Fig. 5 The effect of aminochrome on alpha-tubulin in RCSN-3 cells. The effect of aminochrome on alpha-tubulin in RCSN-3 cells were determined by confocal microscopy. The cells were treated with cell culture medium (**a**); (**b**) 100 μ M dicoumarol; (**c**) 50 μ M aminochrome; and (**d**) 50 μ M aminochrome and 100 μ M dicoumarol during 48 h. The arrows show alpha-tubulin aggregation



regulating vesicle pools by acting as a scaffold to restrict vesicle mobility (Dillon and Goda 2005). Actin is associated with short filaments of synapsin, which are in turn associated to the vesicles (Hirokawa et al. 1989). The actin cytoskeleton regulates the activity of ion channels and transporters involved in maintaining cellular homeostasis and cell volume (Papakonstanti et al. 2000). The reduction in cell volume decrease and loss of the elongated cell shape observed in RCSN-3 cells treated with aminochrome and dicoumarol is probably related to the disruption of the actin filament network.

In mature axons, a network of actin filaments provides stability for membrane integrity, and constitutes a scaffold for short distance transport of molecules. Axonal shape, collateral branching, branch retraction, and axonal regeneration, also depend on actin filament dynamics (Letourneau 2009). Actin filaments also play a role in myosin-dependent mitochondrial movement in axons (Morris and Hollenbeck 1995; Ligon and Steward 2000). A remarkable finding in this study is the morphological change in RCSN-3 cells processes, which communicates these cells, where we could observe a strong immunostaining for actin, probably as a

consequence of aggregation of this protein. According to our results, we cannot state that these processes in RCSN-3 cells correspond to axons or dendrites. However, these results suggest that aminochrome in the presence of dicoumarol can also affect actin-related transport.

Another important component of the cytoskeleton are microtubule, which are composed of similar but not identical subunits of alpha- and beta-tubulin that normally exist in the dimeric form. The dimer is in dynamic equilibrium with microtubules which are, in turn, regulated by GTP, temperature, calcium ion, accessory proteins, and a large number of drugs that modify the state of polymerization and dynamic stability (Wolff 2009). Actin filaments and microtubules polymerize and depolymerize by adding and removing subunits at polymer endings, and these dynamics drive cytoplasmic organization, cell division, and cell motility (Kueh and Mitchison 2009). The cyanobacterial toxin Microcystin-LR induces apoptotic shrinkage associated with the shortening and loss of actin filaments, associated with a concentration-dependent depolymerization of microtubules (Gácsi et al. 2009). Dopamine depletion induced by 6-hydroxydopamine affects transcripts involved

in control of cytoskeletal formation (Krasnova et al. 2007). Also, dopamine induces supernumerary centrosomes and subsequent cell death (Diaz-Corrales et al. 2008). Our results showed that aminochrome, in the presence of dicoumarol, disrupted the alpha- and also the beta-tubulin network observed in control RCSN-3 cells, thus inducing aggregation around the cell membrane. It has been shown that both alpha-synuclein and DAT co-immunoprecipitated with both alpha- and beta-tubulins in the presence of colchicine, vinblastine, or nocodazole, each of which disrupts microtubules or affects microtubule dynamics (Wersinger and Sidhu 2005).

Our results suggest that one of the actions of aminochrome when DT-diaphorase is inhibited is to disrupt the cytoskeleton filament network since actin, alpha-, and beta-tubulin filaments seem to aggregate around the cell membrane when RCSN-3 cells. Proteomic analysis of rat brain mitochondria and SH-SY5Y cell proteins exposed to C¹⁴-dopamine *o*-quinone revealed that this compound form adducts with beta-tubulin and actin, respectively (Van Laar et al. 2009). Dopamine *o*-quinone is the precursor of aminochrome that undergoes spontaneous cyclization to form aminochrome at physiological pH (Segura-Aguilar and Lind 1989). Therefore, it seems to be plausible that these results obtained with proteomic analysis using dopamine *o*-quinone can be interpreted as the ability of aminochrome to form adducts with actin and beta-tubulin since dopamine *o*-quinone is only stable at pH lower than 2 (Segura-Aguilar and Lind 1989).

The present results support the proposed neuroprotective role for DT-diaphorase against aminochrome neurotoxicity (Paris et al. 2007, 2008a, b, 2009b; Segura-Aguilar et al. 2002) in dopaminergic neurons (Schultzberg et al. 1988). DT-diaphorase reduces aminochrome very effectively, preventing aminochrome participation in neurotoxic pathways (one-electron reduction to form the leukoaminochrome *o*-semiquinone radical and adduct formation with alpha-synuclein). DT-diaphorase prevents (i) cell shrinkage, (ii) lost of cell shape, and (iii) disruption of actin, alpha-, and beta-tubulin cytoskeleton networks. The protective effect of DT-diaphorase on actin, alpha-, and beta-tubulin cytoskeleton networks has been studied using the inhibitor dicoumarol which is also able to inhibit complex II, III, and IV of mitochondrial respiration (González-Aragón et al. 2007). However, the incubation of RCSN-3 cells with dicoumarol alone does not induce disruption of actin, alpha-, and beta-tubulin cytoskeleton networks (Figs. 4c, 5b). DT-diaphorase constitutes the 99% of the total quinone reductase activity present in RCSN-3 cells using NADH or NADPH as electron donor. This means that other flavoenzymes that catalyze one-electron reduction of quinones, including NADH/ubiquinone oxidoreductase also called complex I (Zoccarato et al. 2005), are able to reduce

aminochrome to leukoaminochrome *o*-semiquinone radical when DT-diaphorase is inhibited.

In conclusion, our results suggest that aminochrome one-electron reduction metabolism disrupts actin, alpha-, and beta-tubulin filament networks, which are essential for generating and maintaining the elongated cell shape. Actin, alpha-, and beta-tubulin seem to aggregate around the cell membrane, in turn inducing a cell shrinkage that results in a change from an elongated to a spherical shape. In summary, DT-diaphorase protects against aminochrome-induced disruption of cytoskeleton network composed of actin, alpha-, and beta-tubulin.

Acknowledgments This work was supported by FONDECYT #1061083.

References

- Arriagada A, Paris I, Sanchez de las Matas MJ, Martinez-Alvarado P, Cardenas S, Castañeda P, Graumann R, Perez-Pastene C, Olea-Azar C, Couve E, Herrero MT, Caviedes P, Segura-Aguilar J (2004) On the neurotoxicity of leukoaminochrome *o*-semiquinone radical derived of dopamine oxidation: mitochondria damage, necrosis and hydroxyl radical formation. *Neurobiol Dis* 16:468–477
- Baez S, Linderson Y, Segura-Aguilar J (1995) Superoxide dismutase and catalase enhance autoxidation during one-electron reduction of aminochrome by NADPH-cytochrome P-450 reductase. *Biochem Mol Med* 54:12–18
- Bisaglia M, Mammi S, Bubacco L (2007) Kinetic and structural analysis of the early oxidation products of dopamine: analysis of the interactions with alpha-synuclein. *J Biol Chem* 282:15597–155605
- Büchi G, Kamikawa T (1977) An alternate synthesis of 5, 6-dihydroxy-2, 3-dihydroindole-2-carboxylates (cyclodopa). *J Org Chem* 42:4153–4154
- Buchman VL, Ninkina N (2008a) Modulation of alpha-synuclein expression in transgenic animals for modelling synucleinopathies—is the juice worth the squeeze? *Neurotox Res* 14:329–341
- Buchman VL, Ninkina N (2008b) Mouse models for studying function of synuclein family members in the normal and degenerating brain. *Neurotox Res* 13:121
- Cardenas S, Paris I, Fuentes-Bravo P, Graumann R, Riveros A, lozano J, Calegaro M, Caviedes P, Segura-Aguilar J (2008a) DT-diaphorase protection in catecholaminergic cell line against aminochrome neurotoxic effects. *Neurotox Res* 13:120
- Cardenas SP, Perez-Pastene C, Couve E, Segura-Aguilar J (2008b) The DT-diaphorase prevents the aggregation of *a*-synuclein induced by aminochrome. *Neurotox Res* 13:136
- Cingolani LA, Goda Y (2008) Actin in action: the interplay between the actin cytoskeleton and synaptic efficacy. *Nat Rev Neurosci* 9:344–356
- Conway KA, Lee SJ, Rochet JC, Ding TT, Williamson RE, Lansbury PT Jr (2000) Acceleration of oligomerization, not fibrillization, is a shared property of both alpha-synuclein mutations linked to early-onset Parkinson's disease: implications for pathogenesis and therapy. *Proc Natl Acad Sci USA* 97:571–576
- Conway KA, Rochet JC, Bieganski RM, Lansbury PT Jr (2001) Kinetic stabilization of the alpha-synuclein protofibril by a dopamine-alpha-synuclein adduct. *Science* 294:1346–1349
- Diaz-Corrales FJ, Asanuma M, Miyazaki I, Miyoshi K, Hattori N, Ogawa N (2008) Dopamine induces supernumerary centrosomes

- and subsequent cell death through Cdk2 up-regulation in dopaminergic neuronal cells. *Neurotox Res* 14:295–305
- Dillon C, Goda Y (2005) The actin cytoskeleton: integrating form and function at the synapse. *Annu Rev Neurosci* 28:25–55
- Duka T, Sidhu A (2006) The neurotoxin, MPP+, induces hyperphosphorylation of Tau, in the presence of alpha-Synuclein, in SH-SY5Y neuroblastoma cells. *Neurotox Res* 10:1–10
- Fernández CO (2008) Synucleinopathies: structural features and molecular interactions. *Neurotox Res* 13:120
- Fuentes P, Paris I, Nassif M, Caviedes P, Segura-Aguilar J (2007) Inhibition of VMAT-2 and DT-Diaphorase induce cell death in a substantia nigra-derived cell line—an experimental cell model for dopamine toxicity studies. *Chem Res Toxicol* 20:776–783
- Gácsi M, Antal O, Vasas G, Máté C, Borbely G, Saker ML, Gyori J, Farkas A, Vehovszky A, Bánfalvi G (2009) Comparative study of cyanotoxins affecting cytoskeletal and chromatin structures in CHO-K1 cells. *Toxicol In Vitro* 23:710–718
- Gauthier MA, Eibl JK, Crispo JA, Ross GM (2008) Covalent arylation of metallothionein by oxidized dopamine products: a possible mechanism for zinc-mediated enhancement of dopaminergic neuron survival. *Neurotox Res* 14:317–328
- González-Aragón D, Ariza J, Villalba JM (2007) Dicoumarol impairs mitochondrial electron transport and pyrimidine biosynthesis in human myeloid leukemia HL-60 cells. *Biochem Pharmacol* 73:427–439
- Hastings TG (1995) Enzymatic oxidation of dopamine: the role of prostaglandin H synthase. *J Neurochem* 64:919–924
- Hirokawa N, Sobue K, Kanda K, Harada A, Yorifuji H (1989) The cytoskeletal architecture of the presynaptic terminal and molecular structure of synapsin. *J Cell Biol* 108:111–126
- Krasnova IN, Betts ES, Dada A, Jefferson A, Ladenheim B, Becker KG, Cadet JL, Hohmann CF (2007) Neonatal dopamine depletion induces changes in morphogenesis and gene expression in the developing cortex. *Neurotox Res* 11:107–130
- Kueh HY, Mitchison TJ (2009) Structural plasticity in actin and tubulin polymer dynamics. *Science* 325:960–963
- Letourneau PC (2009) Actin in axons: stable scaffolds and dynamic filaments. *Results Probl Cell Differ* 48:65–90
- Liberato D, Byers V, Dennick R, Castagnoli N (1981) Regiospecific attack of nitrogen and sulfur nucleophiles on quinones derived from poison oak/ivy catechols (urushiol) and analogs as models for urushiol-protein conjugate formation. *J Med Chem* 24:28–33
- Ligon LA, Steward O (2000) Role of microtubules and actin filaments in the movement of mitochondria in the axons and dendrites of cultured hippocampal neurons. *J Comp Neurol* 427:351–361
- Morris RL, Hollenbeck PJ (1995) Axonal transport of mitochondria along microtubules and F-actin in living vertebrate neurons. *J Cell Biol* 131:1315–1326
- Norris EH, Giasson BI, Hodara R, Xu S, Trojanowski JQ, Ischiropoulos H, Lee VM (2005) Reversible inhibition of alpha-synuclein fibrillization by dopaminochrome—mediated conformational alterations. *J Biol Chem* 280:21212–21219
- Papakonstanti EV, Vardaki EA, Stournaras C (2000) Actin cytoskeleton: a signaling sensor in cell volume regulation. *Cell Physiol Biochem* 10:257–264
- Paris I, Dagnino-Subiabre A, Marcelain K, Bennett LB, Caviedes P, Caviedes R, Olea-Azar C, Segura-Aguilar J (2001) Copper neurotoxicity is dependent on dopamine-mediated copper uptake and one-electron reduction of aminochrome in a rat substantia nigra neuronal cell line. *J Neurochem* 77:519–529
- Paris I, Martinez-Alvarado P, Cardenas S, Perez-Pastene C, Graumann R, Fuentes P, Olea-Azar C, Caviedes P, Segura-Aguilar J (2005a) Dopamine-dependent iron toxicity in cells derived from rat hypothalamus. *Chem Res Toxicol* 18:415–419
- Paris I, Martinez-Alvarado P, Perez-Pastene C, Vieira MN, Olea-Azar C, Raisman-Vozari R, Cardenas S, Graumann R, Caviedes P, Segura-Aguilar J (2005b) Monoamine transporter inhibitors and norepinephrine reduce dopamine-dependent iron toxicity in cells derived from the substantia nigra. *J Neurochem* 92:1021–1032
- Paris I, Cardenas S, Perez-Pastene C, Lozano J, Graumann R, Riveros A, Caviedes P, Segura-Aguilar J (2007) Aminochrome as preclinical model to study degeneration of dopaminergic neurons in Parkinson's disease. *Neurotox Res* 12:125–134
- Paris I, Lozano J, Cardenas S, Perez-Pastene C, Saud K, Fuentes P, Caviedes P, Dagnino-Subiabre A, Raisman-Vozari R, Shimahara T, Kostrzewska JP, Chi D, Kostrzewska RM, Caviedes P, Segura-Aguilar J (2008a) The catecholaminergic RCSN-3 cell line: a model to study dopamine metabolism. *Neurotox Res* 13:221–230
- Paris I, Mora S, Raisman-Vozari R, Segura-Aguilar J (2008b) Copper neurotoxicity in rat substantia nigra and striatum is dependent on DT-diaphorase inhibition. *Chem Res Toxicol* 21:1180–1185
- Paris I, Lozano J, Perez-Pastene C, Muñoz P, Segura-Aguilar J (2009a) Molecular and neurochemical mechanisms in PD pathogenesis. *Neurotox Res* 16:271–279
- Paris I, Perez-Pastene C, Couve E, Caviedes P, Ledoux S, Segura-Aguilar J (2009b) Copper dopamine complex induces mitochondrial autophagy preceding caspase-independent apoptotic cell death. *J Biol Chem* 284:13306–13315
- Polymeropoulos MH, Lavedan C, Leroy E, Ide SE, Dehejia A, Dutra A, Pike B, Root H, Rubenstein J, Boyer R, Stenoos ES, Chandrasekharappa S, Athanasiadou A, Papapetropoulos T, Johnson WG, Lazzarini AM, Duvoisin RC, Di Iorio G, Golbe LI, Nussbaum RL (1997) Mutation in the alpha-synuclein gene identified in families with Parkinson's disease. *Science* 276:2045–2047
- Riveros A, Cuchillo I, Hanger D, Segura-Aguilar J, Stephenson J (2008) Studies on the effect of the aminochrome treatment in the axonal transport of alpha-synuclein. *Neurotox Res* 13:147
- Schultzberg M, Segura-Aguilar J, Lind C (1988) Distribution of DT-diaphorase in the rat brain: biochemical and immunohistochemical studies. *Neuroscience* 27:763–766
- Segura-Aguilar J, Lind C (1989) On the mechanism of Mn³⁺ induced neurotoxicity of dopamine: prevention of quinone derived oxygen toxicity by DT-diaphorase and superoxide dismutase. *Chem Biol Interact* 72:309–324
- Segura-Aguilar J, Baez S, Widersten M, Welch CJ, Mannervik B (1997) Human class Mu glutathione transferases, in particular isoenzyme M2-2, catalyze detoxication of the dopamine metabolite aminochrome. *J Biol Chem* 272:5727–5731
- Segura-Aguilar J, Metodiewa D, Welch C (1998) Metabolic activation of dopamine o-quinones to o-semiquinones by NADPH cytochrome P450 reductase may play an important role in oxidative stress and apoptotic effects. *Biochim Biophys Acta* 1381:1–6
- Segura-Aguilar J, Diaz-Veliz G, Mora S, Herrera-Marschitz M (2002) Inhibition of DTdiaphorase is a requirement for Mn³⁺ to produce a 6-OH-dopamine like rotational behaviour. *Neurotox Res* 4:127–131
- Segura-Aguilar J, Cardenas S, Riveros A, Fuentes-Bravo P, Lozano J, Graumann R, Paris I, Nassif M, Caviedes P (2006) DT-diaphorase prevents the formation of alpha-synuclein adducts with aminochrome. *Soc Neurosci Abstr* 32:824.17
- Sulzer D, Talloczy Z, Mosharov EM, Martinez-Vicente M, Cuervo AM (2008) Alphasynuclein and autophagy as an early step in Parkinson's disease. *Neurotox Res* 13:120
- Van Laar VS, Mishizen AJ, Cascio M, Hastings TG (2009) Proteomic identification of dopamine-conjugated proteins from isolated rat brain mitochondria and SH-SY5Y cells. *Neurobiol Dis* 34:487–500
- Wersinger C, Sidhu A (2005) Disruption of the interaction of R-synuclein with microtubules enhances cell surface recruitment of the dopamine transporter. *Biochemistry* 44:13612–13624
- Wolff J (2009) Plasma membrane tubulin. *Biochim Biophys Acta* 1788:1415–1433

- Zecca L, Fariello R, Riederer P, Sulzer D, Gatti A, Tampellini D (2002) The absolute concentration of nigral neuromelanin, assayed by a new sensitive method, increases throughout the life and is dramatically decreased in Parkinson's disease. *FEBS Lett* 510:216–220
- Zecca L, Bellei C, Costi P, Albertini A, Monzani E, Casella L, Gallorini M, Bergamaschi L, Moscatelli A, Turro NJ, Eisner M, Crippa PR, Ito S, Wakamatsu K, Bush WD, Ward WC, Simon JD, Zucca FA (2008) New melanic pigments in the human brain that accumulate in aging and block environmental toxic metals. *Proc Natl Acad Sci USA* 105:17567–17572
- Zoccarato F, Toscano P, Alexandre A (2005) Dopamine-derived dopaminochrome promotes H₂O₂ release at mitochondrial complex I: stimulation by rotenone, control by Ca(2+), and relevance to Parkinson disease. *J Biol Chem* 280:15587–15594